possible to show that the hinge-bending motion associated with substrate binding was not viscosity dependent. Unless the hinge bending involves motion of a peptide chain longer than several peptide units (Hass et al., 1978), no viscosity effect is expected.

Overall, we favor mechanism VI with a viscosity-dependent conformation change of the protein. Conformation changes have been shown to accompany transition-state analogue inhibitor binding (Kurz et al., 1985). Furthermore, the nature of this conformation change seems to be independent of the structure of the transition-state analogue (or its affinity). Thus, it seems reasonable to account for the variation in the values of the apparent second-order rate constants for inhibitor binding as the result of differences in the prior-equilibrium binding constants, and for their viscosity dependence as resulting from that of the rate-determining conformation change. However, if this viscosity-dependent structural change is part of the catalytic cycle of the enzyme (which seems likely), then its rate must be substantially greater than the turnover number of the enzyme, $\sim 200\ s^{-1}$, or otherwise we would have detected a greater viscosity effect on V_{max}.

References

Baer, H. P., Drummond, G. I., & Gillis, J. (1968) *Arch. Biochem. Biophys. 123*, 172.

Barshop, B. A., Wrenn, R. F., & Frieden, C. (1983) *Anal. Biochem. 130*, 134.

Beece, D., Bowne, S. F., Czege, J., Eisenstein, L., Frauenfelder, H., Good, D., Marden, M. C., Marque, J., Ormos, P., Reinisch, L., & Yue, K. T. (1981) *Photochem. Photobiol. 33*, 517.

Berg, O. G., & von Hippel, P. H. (1985) *Annu. Rev. Biophys. Biophys. Chem. 14*, 131.

Brouwer, A. C., & Kirsch, J. F. (1982) *Biochemistry 21*, 1302.

Buffel, D. K., McGuigan, C., & Robins, M. J. (1985) *J. Org. Chem. 50*, 2664.

Caldin, E. F. (1964) *Fast Reactions in Solution*, pp 10–11, Wiley, New York.

Cha, S. (1976) *Biochem. Pharmacol. 25*, 2695.

Cleland, W. W. (1977) *Adv. Enzymol. Relat. Areas Mol. Biol. 45*, 273.

Frick, L., Wolfenden, R., Smal, E., & Baker, D. C. (1986) *Biochemistry 25*, 1616.

Frieden, C., Kurz, L. C., & Gilbert, H. R. (1980) *Biochemistry 19*, 5303.

Hardy, L. W., Kirsch, J. F. (1984) *Biochemistry 23*, 1275.

Hass, E., Katchalski-Katzir, E., & Steinberg, I. Z. (1978) *Biopolymers 17*, 11.

Hiromi, K. (1979) *Kinetics of Fast Enzyme Reactions*, p 258, Halsted Press (Wiley), New York.

Kurz, L. C., & Frieden, C. (1983) *Biochemistry 22*, 382.

Kurz, L. C., LaZard, D., & Frieden, C. (1985) *Biochemistry 24*, 1342.

Marquardt, D. W. (1963) *J. Soc. Ind. Appl. Math 2*, 431.

Murphy, P. M., Noonan, M., Collins, P., Tully, E., & Brady, T. G. (1969) *Biochim. Biophys. Acta 171*, 157.

Pauling, L. (1946) *Chem. Eng. News 24*, 1375.

Shimazaki, M., Nakamura, H., Ihaka, Y., & Ohno, M. (1983) *Chem. Pharm. Bull. 31*, 3104.

Stokes, R. H., & Weeks, I. A. (1964) *Aust. J. Chem. 17*, 304.

Tsong, T. Y. (1982) *Biochemistry 21*, 1493.

Wolfenden, R. (1968) *Biochemistry 7*, 2409.

Wolfenden, R. (1972) *Acc. Chem. Res. 5*, 10.

Wolfenden, R. (1976) *Annu. Rev. Biophys. Bioeng. 5*, 271.

Wolfenden, R., Wentworth, D. F., & Mitchell, G. N. (1977) *Biochemistry 16*, 5071.

Electronic Probes of the Mechanism of Substrate Oxidation by Buttermilk Xanthine Oxidase: Role of the Active-Site Nucleophile in Oxidation†

Edward B. Skibo,* James H. Gilchrist, and Chang-Hee Lee

Department of Chemistry, Arizona State University, Tempe, Arizona 85287

Received September 26, 1986; Revised Manuscript Received January 15, 1987

ABSTRACT: Quinazolin-4(3*H*)-one derivatives substituted at the 6- and/or 7-position were studied as electronic probes of substrate oxidation by buttermilk xanthine oxidase. Since the enzyme active site possesses dimensional tolerance, the substituents exert an electronic effect rather than a steric effect on the catalytic parameters for oxidation. This feature permitted a Hammett plot to be made for quinazoline–oxygen substrate activity. The concave downward nature of this plot indicates that the rate-determining step for oxidation changes when electron-withdrawing substituents are placed on the substrate. This plot and kinetic isotope effects obtained with 2-deuterio derivatives of the substrates indicate the following: (i) oxidation involves nucleophile transfer to the C(2) center in concert with hydride transfer to the molybdenum center, and (ii) the formation of oxidized product is a three-step process, i.e., Michaelis complex formation, oxidation, and hydrolysis of the oxidized substrate–enzyme adduct. The role of the nucleophile in oxidation appears to be to increase the electron density in the substrate and thereby facilitate hydride transfer. The implication of this study is that similar electronic probes may be designed to study other purine-utilizing enzymes possessing a dimensionally tolerant active site.

Buttermilk xanthine oxidase is a complex molybdenum-containing enzyme that oxidizes a variety of substrates including hydroxypurines and quinazolines (Bray, 1975, pp 346–349; Krenitsky et al., 1972). The catalytic mechanism of oxidation is thought to involve hydride transfer (or its equivalent) from the substrate in concert with nucleophile transfer to the substrate (Stiefel, 1973; Edmondson et al., 1973;

† This research was supported by an award from the National Cancer Institute, DHHS (PHS 1R01 CA36876-03).

0006-2960/87/0426-3032$01.50/0

Olson et al., 1974; Bray et al., 1979). The essential features of the mechanism proposed by Bray et al., (1979) are shown in eq 1. The nucleophile X^- has been proposed to be a ter-

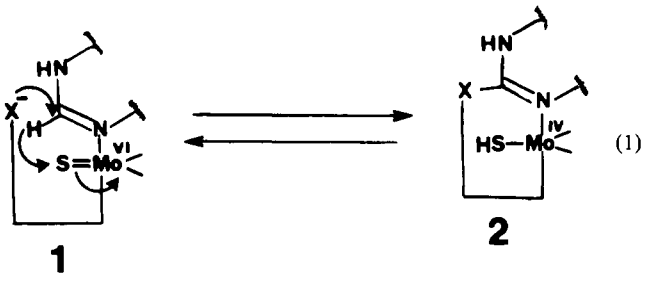

(1)

minal oxo group on the molybdenum center (Gutteridge & Bray, 1980; Bray & Gutteridge, 1982) but is depicted as found in eq 1 for convenience. In spite of the large number of studies, the detailed mechanism of nucleophile-assisted substrate oxidation is as yet unreported [for a recent review of the enzyme, see Hille and Massey (1985)]. Described in this paper is a mechanistic study of this process utilizing quinazoline electronic probes and isotope effects. Our results suggest that a concerted nucleophile–hydride transfer does occur, but with hydride transfer lagging behind nucleophile transfer resulting in a partial negative charge in the substrate during oxidation. Thus, the nucleophile appears to facilitate hydride transfer by increasing the electron density in the substrate. This study also provides evidence of a three-step process leading to oxidized substrate: Michaelis complex formation, oxidation, and hydrolysis of the oxidized substrate–enzyme adduct. The enzymatic oxidations of xanthine (Olson et al., 1974) and lumazine (Davis et al., 1982, 1984) are likewise proposed to occur by this three-step process. The implication of this study goes beyond the mechanism of substrate oxidation by xanthine oxidase, however; the method described may be used to study other purine-utilizing enzymes having a dimensionally tolerant active site.

Provided in eq 2 are the quinazoline electronic probes

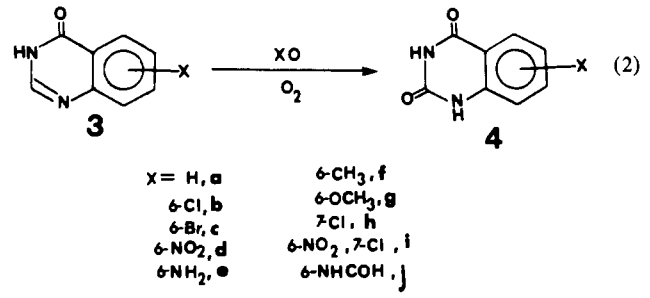

(2)

studied as substrates of the enzyme. Leonard et al. (1975) and Leonard (1982) have observed that the xanthine oxidase active site tolerates dimensionally altered substrates such as imidazo[4,5-*g*]quinazolines. This observation suggests that the substrate–oxygen reductase activity of quinazolines bearing a substituent in the 6- and/or 7-position would be influenced largely by the electronic effect of the substituent rather than by steric effects. This proved to be correct, and a Hammett plot was obtained for quinazoline–oxygen reductase activity. The change in slope exhibited by this plot and kinetic isotope effects provide the bases for the conclusions of this study. Since the compounds in eq 2 are employed as probes of the electronic structure of intermediates present during catalysis, they have been termed electronic probes. Leonard (1982) has noted that many other purine-utilizing enzymes exhibit a dimensional tolerance for substrates. Thus, imidazo[4,5-*g*]quinazoline derivatives of endogenous purine substrates act as substrates in many cases. Recently, we have succeeded in functionalizing this system with substituents at the 4-position (Lee et al., 1986; C. H. Lee, et al., unpublished results). The possibility that these derivatives could act as electronic probes is currently being investigated.

Materials and Methods

All kinetic measurements were carried out on either a Perkin-Elmer 559 spectrometer or Perkin-Elmer Lambda-3 spectrometer in which the cell holder had been maintained at 30.0 ± 0.2 °C by circulating thermostated water. UV–visible spectra were obtained on a Perkin-Elmer 559 spectrometer with μ = 1.0 (KCl) aqueous buffer as solvent. Uncorrected melting points were determined with a Mel-Temp apparatus. Elemental analyses were performed by MicAnal Laboratories, Tucson, AZ. Thin-layer chromatographies (TLCs) were run with Merck silica gel 60 (f_{254}) plates. IR spectra were taken as KBr pellets with a Nicolet MX-1 FTIR spectrophotometer; only the wavelengths of intense bands are tabulated. ^{1}H NMR spectra were taken on a Bruker WH-90 spectrometer. Measurements of pH were made with a Radiometer PHM 84 pH meter equipped with a Radiometer GK2401C combination electrode.

Buttermilk xanthine oxidase, grade III, was purchased from Sigma Chemical Co. The formamide-*d* (99.2% D) employed in the synthesis of deuteriated substrates was purchased from MSD Isotopes. The inorganic salts used in the preparation of buffer solutions were of analytical reagent grade obtained from Mallinkrodt and were used as such. The buffer solutions were prepared in doubly glass-distilled water.

Quinazolines **3a–h** (Baker et al., 1952) and **3i** (Leonard et al., 1975) were prepared as previously described. Quinazoline **3j** was prepared by formylation of **3e**, and the 2-deuterio derivatives of **3b**, **3d**, and **3f** were prepared by fusion of the appropriate anthranilic acid with deuteriated formamide.

Described below are the preparations of the unreported derivative **3j** and the 2-deuterioquinazoline derivatives.

6-Formamidoquinazolin-4(3H)-one (**3j**). A solution of 750 mg (3.79 mmol) of **3e** hydrochloride salt in 25 mL of water was adjusted to pH 3 with formate buffer. Evaporation of the water in vacuo afforded a mixture of the formate salt of **3e** and other salts. Addition of 20 mL of formic acid (88%) and 6 mL of acetic anhydride to these solids was followed by stirring at room temperature for 2 min. The reaction was then heated until boiling occurred and allowed to cool to room temperature. Evaporation of the reaction mixture to dryness followed by additiion of water resulted in crystallization of 250 mg (35%) of crude **3j**. Recrystallization was carried out from methanol–ethyl acetate (1:9): mp 268–270 °C dec; TLC (6% methanol in chloroform) on silica gel, R_f 0.09; IR (KBr) 3565, 3480, 3239, 3057, 2868, 1678, 1662, 1595, 1484, 1391 cm^{-1}; ^{1}H NMR (dimethyl-d_6 sulfoxide) δ 8.32 (1 H, d, J = 1.6 Hz, formyl proton coupled with N–H), 8.01 [1 H, s, C(2)–H], 8.5–7.6 [3 H, complex splitting of C(5), C(7), and C(8) protons]. The ^{1}H NMR spectrum indicates that a minor amount of the 6-acetamido derivative is present. Anal. Calcd for $C_9H_7N_3O{\cdot}0.75H_2O$: C, 53.32; H, 4.22; N, 20.72. Found: C, 53.59; H, 3.79; N, 20.88.

2-Deuterio Derivatives of **3b** *and* **3f** (**3b**-*2-d and* **3f**-*2-d*). A mixture of the appropriate anthranilic acid (1 mmol) and formamide-*1-d* (2 mmol) was treated with CH_3OD to remove exchangeable protons: addition of 5 mL of CH_3OD followed by evaporation to dryness was carried out 3 times. We have observed that the 1-deuterio group of formamide exchanges with protons during the fusion described below. The CH_3OD treatments thus serve to ensure that there is >90% deuterium incorporation at the 2-position of the product. Fusion of the

dried reaction mixture at 180 °C was carried out until the melt solidified, usually after a 1-h reaction time. The solids were then triturated with methanol and filtered. Recrystallization of the product was carried out from either methanol or chloroform/hexane. ^{1}H NMR spectra of the purified products revealed that the C(2) proton usually found at δ 8.1 was absent.

2-Deuterio Derivative of **3d** (**3d-2-d**). **3a-2-d** was prepared from anthranilic acid by the method described above. Nitration of this compound was carried out as previously described for the nondeuteriated derivatives (Baker et al., 1952). The product was purified by recrystallization from acetic acid.

Product Studies. The quinazolines all show a high degree of substrate inhibition, and thus preparative studies were not possible except at high dilution. Authentic oxidation products were prepared as previously described (Armarego, 1967); UV–visible spectral comparisons of these with enzymatic oxidation products indicated that the expected products had formed in quantitative yield.

pK_a determinations were carried out spectrophotometrically in aqueous buffer (μ = 1.0 with KCl) at 30 °C. The pK_a value was obtained by computer fitting absorbance vs. pH data to $OD = (A_T a_H \epsilon_{HA} + A_T \epsilon_A K_a)/(a_H + K_a)$, where A_T is the total concentration of added compound, ϵ_{AH} is the extinction coefficient of the acid form, ϵ_A is the extinction coefficient of the base form, and K_a is the acid dissociation constant. The error in pK_a values ranges from ±0.01 to ±0.05 pK_a unit.

Determination of Substrate–Oxygen Reductase Activity. The activity of quinazoline substrates was studied in 0.05 M pH 7.40 phosphate buffer (μ = 0.1, KCl) containing 22 μM EDTA at 30 °C. The concentration of xanthine oxidase employed ranged from 0.027 to 0.27 μM (per enzyme-bound FAD); molarities were determined from an absorbance measurement at 450 nm and the ϵ_{450} value of 37 800 M^{-1} cm^{-1} per enzyme-bound FAD (Massey et al., 1969). High concentrations of enzyme were employed when the substrate turnover number was very small. Thereby, the reaction could be followed over short periods of time without concomitant enzyme denaturation. Initial velocities were obtained at the λ_{max} value of the substrate (between 260 and 280 nm); $\Delta\epsilon$ values for oxidation in this wavelength range are typically 5000–10 000 M^{-1} cm^{-1}. The catalytic parameters were obtained from Lineweaver–Burk plots with five to seven data points. For the calculation of isotope effects, the average catalytic parameters from two such plots were employed. Errors in apparent k_{cat} and K_m values ranged from 15 to 20%.

Results

Compounds **3a–j** were examined as substrates of buttermilk xanthine oxidase with 0.027–0.27 μM enzyme in 0.05 M pH 7.40 phosphate buffer (μ = 0.1, KCl) at 30 °C. All compounds were quantitatively oxidized to the respective dione derivatives **4a–j** as verified by comparisons of final UV–visible spectra with those of authentic compounds. Lineweaver–Burk plots for substrate–oxygen reductase activity indicated that the substrates are capable of inhibiting the enzyme at high concentrations, Figure 1. Indeed, preparative reactions failed to provide any oxidation products except when carried out at high dilution. The apparent values of K_m and k_{cat} for substrate–oxygen reductase activity found in Table I were obtained from Lineweaver–Burk plots of low-substrate data as shown in Figure 1.

Xanthine also inhibits the enzyme when present at high concentrations, probably as a result of the formation of an inactive substrate–enzyme–substrate complex (Hofstee, 1955). The presence of such a complex suggests that the apparent

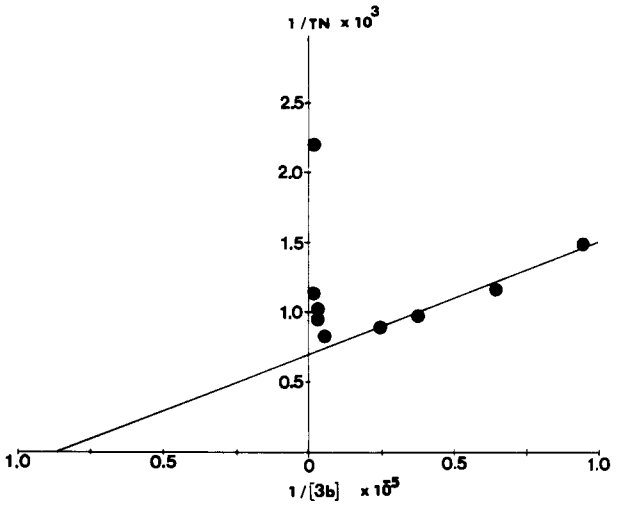

FIGURE 1: Plot of 1/turnover number vs. 1/[**3b**] for the oxidation of **3b** in 0.05 M pH 7.4 phosphate buffer (μ = 0.1, KCl) at 30 °C.

Table I: pK_a Values and Catalytic Parameters for Oxidation of Quinazoline Substrates

substrate	pK_a value[a]	apparent k_{cat} (min^{-1})	apparent K_m (×10^5 M)
3a	9.67	24	5.5
3b	9.37	1663	2.27
3c	9.17	1331	1.15
3d	8.43	1133	0.63
3e	10.40	1.2	3.3
3f	9.8	144	7.46
3g	9.75	228	10.8
3h	9.32	491	1.58
3i	8.10	322	0.26
3j	9.36	684	5.00

[a] Acid dissociation of the N(3) proton.

values of K_m and k_{cat} found in Table I contain binding constants not involved in product formation (vide infra, Discussion). Thus the observed changes in these parameters with the electronic character of the substituent could be due to changes in productive as well as nonproductive constants. Indeed, a Hammett plot obtained with k_{cat} values (not shown) exhibits a high degree of scatter. In order to focus exclusively on equilibria and first-order processes involved in product formation, the Hammett plot was obtained with the ratio apparent k_{cat}/K_m. This ratio is unaffected by both nonproductive binding and the accumulation of intermediates (Fersht, 1979) and is equal to the product of equilibrium and first-order constants involved in product formation (vide infra, Discussion).

Found in Figure 2 is the Hammett plot for the oxidation of quinazoline substrates. The pK_a values for acid dissociation from the pyrimidine N–H group of the substrates were used in place of Hammett σ values for determining the electronic effect of substituents. As shown in eq 3 for a substituted

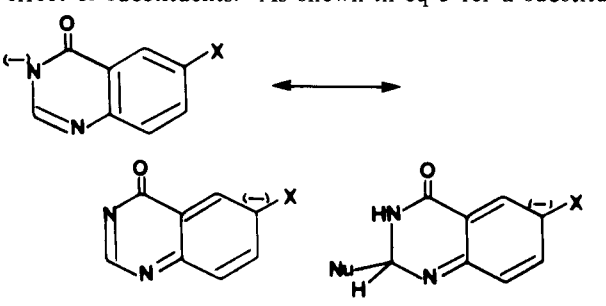

(3)

quinazoline, the anion arising from N(3)–H acid dissociation

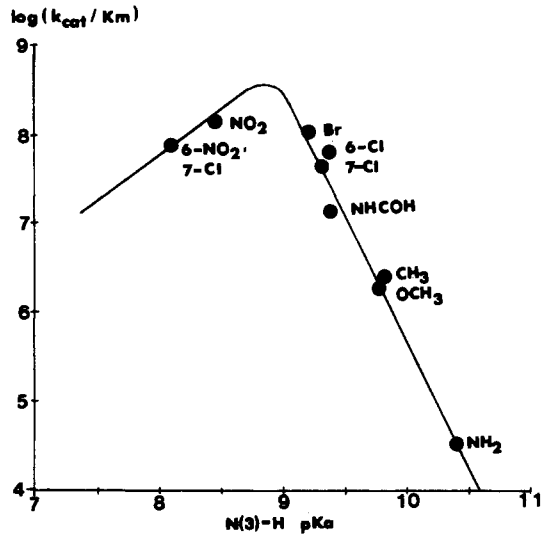

FIGURE 2: Plot of log (k_{cat}/K_m) vs. the pK_a of the N(3) proton of substrates **3**. The catalytic parameters were obtained in 0.05 M pH 7.4 phosphate buffer (μ = 0.1, KCl) at 30 °C.

has the same distribution as the anion resulting from nucleophile transfer to the 2-position. The relative pK_a values of the substrates thus provide a measure of the relative stability of the corresponding anionic adducts. The use of pK_a values instead of σ values permits a convenient assessment of electronic effects regardless of the substituent's location and deviation from coplanarity with the benzene ring (as may be the case with **3i**). In all cases, the pK_a values indicate that the substrates exist in >90% as the neutral species at the pH value employed for these studies. Thus, all reactions are considered to involve the neutral substrate. The use of apparent k_{cat}/K_m would, however, cancel out any acid dissociation terms in the individual catalytic constants.

An important consideration is the possible steric influence of substituents on the values of apparent k_{cat}/K_m. It appears that the electronic effect of substituents, as measured by pK_a values, is largely responsible for the observed changes in these values. In **3b** and **3h**, for example, the steric bulk of the chloro substituent is moved to another position on the quinazoline ring without changing the pK_a or apparent k_{cat}/K_m values substantially. Another example is **3j**: the formamido substituent of this substrate is larger than most of the other substituents and is capable of hydrogen bonding, but the corresponding datum still falls on the curve in Figure 2. The only anomalous datum is that obtained from **3a**, which deviates widely from the plot and has been left out. Such errant data points are not uncommon on Hammett plots (Hammett, 1970). The deviations of the 6-nitro and 7-chloro-6-nitro derivatives are proposed to be systematic in nature, however. This assessment is based on the observation that kinetic isotope effects parallel these deviations (vide infra).

Inspection of Figure 2 reveals that the Hammett plot of substrates with pK_a values >9 is linear (correlation coefficient = 0.98) with a slope of −2.86. Substrates with electron-withdrawing substituents, pK_a values <9, appear to fall on another linear plot with a slope of +1. The change in slope is due to a change in the rate-determining step by virtue of the concave downward nature of the Hammett plot (Sykes, 1981). To provide further insight into the mechanisms involved, kinetic isotope effects were obtained at the two linear regions of the plot (Table II). Inspection of both tables reveals that apparent K_m experiences small kinetic isotope effects in both linear regions. These effects are small enough to be within the bounds of experimental error (±15–20% in K_m determinations). Thus, apparent K_m is probably not actually experiencing an isotope effect. Apparent k_{cat}, on the other hand, experiences large kinetic isotope effects in the electron-releasing (pK_a > 9) linear region and no kinetic isotope effect in the electron-withdrawing (pK_a < 9) linear region. The isotope studies suggest that the rate-determining step is switching from substrate oxidation (subject to kinetic isotope effects) to oxidized adduct hydrolysis (not subject to kinetic isotope effects). This interpretation is consistent with the three-step process proposed by Olson (1974) and Davis et al. (1982, 1984) for substrate oxidation (vide infra, Discussion).

Table II: Kinetic Isotope Effects

substrate	apparent k_{cat} (min^{-1})	apparent K_m (×10^5 M)	KIE[a]
3b-*2-d*	767	3.17	3.0
3f-*2-d*	41.3	11.1	5.2
3d-*2-d*	992	0.47	1.1

[a] Ratio of apparent k_{cat}/K_m values for protio and deuterio derivatives.

Scheme I

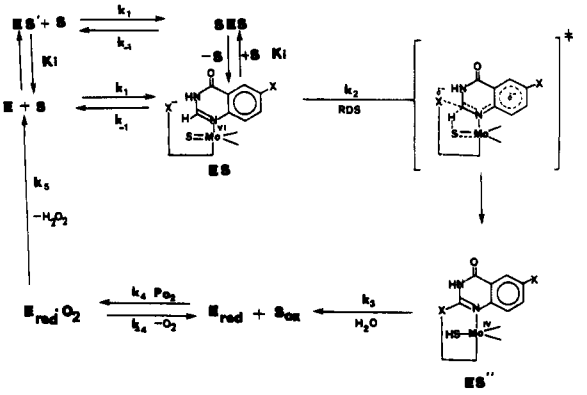

Discussion

The results cited above are discussed in conjunction with the mechanism found in Scheme I. The formation of oxidized product is postulated to occur by the three-step process: Michaelis complex formation (ES), oxidation, and hydrolysis of the adduct ES''. The oxidation process ES → ES'' is proposed to occur by a concerted nucleophile–hydride transfer mechanism.

Some of the features found in Scheme I are derived from other studies. For example, the presence of nucleophile X^- and the structure of the molybdenum center are based on the mechanism postulated by Bray et al. (1979) and Bray (1980). This study indicates the role that X^- plays in catalysis but does not provide additional insights into the structure of the molybdenum center. Another feature is noncompetitive formation of the inactive complexes ES' and SES on the basis of Hofstee's (1955) studies of xanthine inhibition of the enzyme. It was suggested by Hofstee (1955) that the inactivity of SES is due to interference by the second bound substrate with oxygen binding at the FAD cofactor. Supportive of this suggestion is the observation that benzimidazole analogues inhibit the enzyme by binding at or near the functional FAD cofactor (Skibo, 1986). Thus, the binding site of the substrate in ES' and the second bound substrate of SES may be at or near this cofactor. It should be pointed out that inhibition at high substrate concentrations has also been attributed to overreduction of the enzyme (Hille & Steward, 1984; Morpeth, 1983). Hille and Steward (1984) suggested that high substrate concentrations favor the formation of an inactive complex

consisting of reduced enzyme and substrate. Morpeth (1983), on the other hand, suggested that substrate inhibition is due to the slow release of oxidized product from the overreduced enzyme. However, the noncompetitive formation of inactive complexes shown in Scheme I is supported by the following observations: (i) substrate inhibition occurs regardless of the rate-determining step (oxidation or release of oxidized product), and (ii) the Hammett plot obtained with k_{cat} is highly scattered, probably due to substituent effects on the noncompetitive binding constant K_i and other parameters (vide infra). Preliminary results (E. B. Skibo, unpublished results) indicate that substituent effects on quinazoline oxidation and substrate inhibition are quite different, suggesting that the latter involves substrate binding to a site other than at the molybdenum center.

Evidence for the oxidation mechanism in Scheme I is provided by the linear plot in Figure 2 at pK_a values >9 and the isotope studies in this region, **3b**-*2-d* **3f**-*2-d* in Table II. Application of the steady-state approximation to the mechanism in Scheme I provides the expression for the reciprocal plots found in eq 4. At high substrate concentrations, the last term

$$\frac{1}{TN} = \frac{k_3k_5 + k_2k_5 + k_2k_3}{k_3k_2k_5} + \frac{k_{-1} + k_2}{k_2k_1K_i} + \frac{1}{P_{O_2}}\frac{k_5 + k_4}{k_4k_5} + \frac{1}{[S]}\frac{k_{-1} + k_2}{k_1k_2} + \frac{[S]}{k_2K_i} \quad (4)$$

of this expression prevails, and the turnover number (TN) decreases with increasing substrate concentration as shown in Figure 1. At low substrate concentrations and constant P_{O_2}, the relationship is linear with slope = apparent $K_m/k_{cat} = (k_{-1} + k_2)/k_1k_2$. Approximate expressions for the catalytic parameters could be obtained with the following inequalities: (i) k_2 is rate determining; thus, $k_2 < k_3$. (ii) Substrate and oxygen binding are rapid, and consequently, k_1, k_{-1}, k_4, and k_{-4} are greater than any other rate constants. (iii) Reoxidation is rapid, and $k_5 > k_2$ and k_3. The latter two inequalities hold for xanthine–oxygen reductase activity (Olson et al., 1974). The presence of kinetic isotope effects suggests that substrate and oxygen binding as well as reoxidation are also nonrate determining during quinazoline–oxygen reductase activity. The catalytic parameters are now as follows: apparent $k_{cat}/K_m = k_1k_2/k_{-1}$; apparent $k_{cat} = k_1k_2K_i/(k_1K_i + k_{-1})$, and apparent $K_m = K_ik_{-1}/(k_1K_i + k_{-1})$.

According to the proposed mechanism in Scheme I, the plot of log (k_{cat}/K_m) vs. the N(3)–H pK_a value at pK_a values >9 is a measure of the substituent effect on k_1k_2/k_{-1}. The expression k_1/k_{-1} pertains to equilibrium formation of the Michaelis complex ES, which presumably involves ligation of the N(1) lone pair to the molybdenum center. The lone pair is not in direct conjugation with the substituents and thus should only experience inductive electronic effects. The process represented by k_2, on the other hand, results in the development of an anion having the same distribution as the anion arising from N(3)–H acid dissociation (see eq 3). Factors that increase this acid dissociation constant should proportionally lower the activation energy associated with k_2. The negative slope of the Hammett plot (pK_a values >9) in Figure 2 indicates that this is indeed the case.

Kinetic isotope effects measured for substrates found on the electron-releasing (pK_a >9) linear plot are consistent with hydride transfer occurring in concert with nucleophile transfer. The expression for apparent k_{cat} provided above contains k_2 and should therefore be subject to kinetic isotope effects, if the mechanism in Scheme I is correct. The kinetic isotope effects on apparent k_{cat} for the oxidation of substrates **3b** and **3f** are large (from 3.5 to 4.6), consistent with a hydride-transfer process. The apparent K_m expression, on the other hand, contains only constants involved in equilibrium binding, and thus this parameter is not subject to these effects.

Clearly, the results discussed above indicate that the mechanism often suggested for substrate oxidation, carbocation formation by hydride transfer from the substrate followed by nucleophile trapping, is not correct. The process represented by k_2 in Scheme I parallels a well-known reaction in organic chemistry: hydride transfer from an anionic species. Examples include the Cannizzaro reaction (March, 1985), the oxidation of methoxide (Swain et al., 1979; Skibo & Lee, 1985), and hydride transfer from a carbanion to carbalumiflavin (Farng & Bruice, 1984).

The change in slope observed at pK_a values <9 in Figure 2 is likely due to a change in the rate-determining step from oxidation to adduct breakdown. This change was expected since the process represented by k_2 should become very faborable when electron-withdrawing substituents are present. The assessment that adduct breakdown (k_3) is rate determining comes entirely from kinetic isotope effects. Before these effects are discussed, the meaning of the apparent k_{cat} and K_m values must be elaborated upon. It is obvious from the rate law in eq 4 that simply changing the rate-determining step from k_2 to k_3 will not affect the apparent k_{cat}/K_m value. To explain the change in slope, oxidation is proposed to become a reversible process represented by $K_2 = k_2/k_{-2}$. Application of the steady-state approximation and assuming that substrate and oxygen binding, as well as reoxidation, are non rate determining processes provides the following expressions: apparent $k_{cat}/K_m = k_1K_2k_3/k_{-1}$; apparent $k_{cat} = k_3k_1K_2K_i/(k_{-1} + k_1K_i + k_1K_2K_i)$; apparent $K_m = K_iK_{-1}/(k_{-1} + k_1K_i + k_1K_2K_i)$.

The kinetic isotope effect on K_2 is expected to be small or negligible since the individual effects on k_2 and k_{-2} would tend to cancel. Adduct breakdown (k_3) should, of course, experience no kinetic isotope effects. Thus, the value of apparent k_{cat} should not change very much upon deuteriation, particularly if the K_2-containing term is larger than the other terms in the denominator. The value of apparent K_m, on the other hand, would either increase slightly or remain the same depending on whether the K_2-containing term predominates or is relatively small in the denominator, respectively. In accord with these predictions, kinetic isotope effects on apparent k_{cat} and K_m for **3d** oxidation are negligible. The results of kinetic isotope studies on xanthine–oxygen reductase activity carried out by Edmondson et al. (1973) are also in accord with these predictions. Xanthine, like the substrates **3d** and **3i**, is postulated to have adduct breakdown as the rate-determining step, and the effect of 8-deuteriation on xanthine–oxygen reductase activity is to increase K_m while leaving k_{cat} unchanged. It should be pointed out, however, that in a followup publication Olson et al. (1974) discussed this result in terms of a decrease in K_m although Figure 11 of Edmondson et al. (1973) clearly shows the opposite effect.

The expression for apparent $k_{cat}/K_m = k_1K_2k_3/k_{-1}$ obtained above differs from the expression derived for the electron-releasing linear plot. Thereby, the observed change in slope of the Hammett plot could be explained. As noted earlier, apparent k_{cat}/K_m is independent of the accumulation of intermediates, and changing the rate-determining step from k_2 to k_3 in Scheme I will have no effect on this ratio. The substituent effect on the new expression for k_{cat}/K_m pertains to the product of substituent effects on k_1/k_{-1}, K_2, and k_3. The positive slope of the Hammett plot may be the result of

rate-determining adduct hydrolysis involving electron loss from the substrate. A possible mechanism is rapid equilibrium addition of water at the C(2) center followed by rate-determining elimination of nucleophile X^-.

Conclusions

It is concluded that quinazolines, like xanthine and lumazine substrates, form oxidation products by the three-step process: Michaelis complex formation, oxidation, and hydrolysis of the oxidized adduct. Now that this process has been documented for three diverse substrates, we are tempted to conclude that it is in operation for other substrate systems as well. It is also concluded that oxidation involves nucleophile transfer to the C(2) center in concert with hydride transfer to the molybdenum center. Thus, the nucleophile increases the electron density in the substrate and thereby facilitates the hydride transfer. Hydride transfer, however, has not been rigorously distinguished from an equivalent process such as sequential hydrogen atom and electron transfer. Finally, we conclude that similar mechanistic studies could be carried out on other purine-utilizing enzymes with a dimensionally tolerant active site.

References

Armarego, W. L. F. (1967) in *Quinazolines* (Brown, D. J., Ed.) Part 1, pp 202–203, Interscience, New York.

Baker, B. R., Schaub, R. E., Joseph, J. P., McEvoy, F. J., & Williams, J. H. (1952) *J. Org. Chem. 17*, 141.

Bray, R. C. (1975) *Enzymes (3rd Ed.) 12*, 299–419.

Bray, R. C. (1980) in *Biological Magnetic Resonance* (Berliner, L. J., & Reuben, J., Eds.) pp 45–84, Plenum, New York.

Bray, R. C., & Gutteridge, S. (1982) *Biochemistry 21*, 5992–5999.

Bray, R. C., Gutteridge, S., Stotter, D. A., & Tanner, S. J. (1979) *Biochem. J. 177*, 357–360.

Davis, M. D., Olson, J. S., & Palmer, G. (1982) *J. Biol. Chem. 257*, 14730–14737.

Davis, M. D., Olson, J. S., & Palmer, G. (1984) *J. Biol. Chem. 259*, 3526–3533.

Edmondson, D. B., Ballou, D., Van Heuvelen, A., Palmer, G., & Massey, V. (1973) *J. Biol. Chem. 248*, 6135–6144.

Farng, O. L., & Bruice, T. C. (1984) *J. Chem. Soc., Chem. Commun.*, 185–186.

Fersht, A. (1977) *Enzyme Structure and Mechanism*, p 91, Freeman, San Francisco.

Gutteridge, S., & Bray, R. C. (1980) *Biochem. J. 189*, 615–623.

Hammett, L. P. (1970) *Physical Organic Chemistry*, 2nd ed., pp 365–366, McGraw-Hill, New York.

Hille, R., & Stewart, R. C. (1984) *J. Biol. Chem. 259*, 1570–1576.

Hille, R., & Massey, V. (1985) in *Molybdenum Enzymes* (Spiro, T. G., Ed.) pp 443–518, Wiley-Interscience, New York.

Hofstee, B. H. J. (1955) *J. Biol. Chem. 216*, 235–244.

Krenitsky, T. A., Neil, S. M., Elion, G. B., & Hitchings, G. H. (1972) *Arch. Biochem. Biophys. 150*, 585–599.

Lee, C. H., Gilchrist, J. H., & Skibo, E. B. (1986) *J. Org. Chem. 51*, 4784–4792.

Leonard, N. J. (1982) *Acc. Chem. Res. 15*, 128–135.

Leonard, N. J., Morrice, A. G., & Sprecker, M. A. (1975) *J. Org. Chem. 40*, 356–363.

Leonard, N. J., Sprecker, M. A., & Morrice, A. G. (1976) *J. Am. Chem. Soc. 98*, 3987–3994.

March, J. (1985) *Advanced Organic Chemistry*, 3rd ed., pp 1117–1119, Wiley, New York.

Massey, V., Brumby, P. E., Komai, H., & Palmer, G. (1969) *J. Biol. Chem. 244*, 1682–1691.

Morpeth, F. F. (1983) *Biochim. Biophys. Acta 744*, 328–334.

Olson, J. S., Ballou, D. P., Palmer, G., & Massey, V. (1974) *J. Biol. Chem. 249*, 4363–4382.

Skibo, E. B. (1986) *Biochemistry 25*, 4189–4194.

Skibo, E. B., & Lee, C. H. (1985) *J. Am. Chem. Soc. 107*, 4591–4593.

Stiefel, I. E. (1973) *Proc. Natl. Acad. Sci. U.S.A. 70*, 988–992.

Swain, C. G., Powell, A. L., Lynch, T. J., Alpha, S. R., & Dunlap, R. P. (1979) *J. Am. Chem. Soc. 101*, 3584–3587.

Sykes, P. (1981) *Guidebook to Mechanism in Organic Chemistry*, 5th ed., pp 366–369, Longman, New York.